Acta Cryst. (1984). B40, 398–404

Theoretical and Experimental Studies of the Charge Density in Urea

BY S. SWAMINATHAN AND B. M. CRAVEN

Department of Crystallography, University of Pittsburgh, Pittsburgh, PA 15260, USA

AND M. A. SPACKMAN† AND R. F. STEWART

Department of Chemistry, Carnegie–Mellon University, Pittsburgh, PA 15213, USA

(*Received 7 October 1983; accepted 20 January 1984*)

Abstract

X-ray structure amplitudes $|F_o^x|$ for urea at 123 K have been derived experimentally for 318 reflections, $|F| > 3\sigma(F_o)$, $\sin\theta/\lambda < 1{\cdot}15$ Å^{-1}. Corresponding amplitudes $|F_o^t|$ have also been calculated for a simulated crystal structure with the charge density derived from a 6-31G** wavefunction for the isolated urea molecule. The nuclear positional and anisotropic thermal parameters at 123 K were those obtained by neutron diffraction. The $|F_o^x|$ were placed on an 'absolute' scale with the $|F_o^t|$. Simple pseudoatom models for the charge density have been fitted by least squares using the set of $|F_o^x|$ and $|F_o^t|$ as observations in separate refinements. Maps of the resulting static deformation density distribution are similar to each other and to the map derived directly from the wavefunction. Thus the pseudoatom models are efficient, although there are limitations which are attributed primarily to the restricted nature of the radial functions. The most significant differences between the experimental and theoretical model maps are close to the H atoms and may be related to H-bonding effects in the crystal. [Crystal data: $a = 5{\cdot}578(1)$, $c = 4{\cdot}686(1)$ Å, tetragonal, $P\bar{4}2_1m$ with two molecules per unit cell lying in special positions having point symmetry $2mm$.]

Introduction

Urea has been reinvestigated as part of a study of the charge density distribution in amide groups. Urea was chosen because the crystal and molecular structures are simple, allowing detailed comparisons to be made of the charge distributions obtained from accurate diffraction data and from *ab initio* quantum-chemical calculations. Recently, the charge density distribution in urea was determined from X-ray data collected at 123 K and analysed with two different structure factor models (Mullen & Hellner, 1978; Mullen, 1980). There were notable differences from the theoretical charge distribution calculated with a 4-31G basis set by Scheringer, Mullen, Hellner, Hase, Schulte & Schweig (1978). With more extensive X-ray data collected at 123 K and by making use of the 123 K neutron structure of Swaminathan, Craven & McMullan (1984*a*), hereafter SCM, we have obtained an experimental charge density distribution differing from that which is cited above, but in satisfactory agreement with an SCF theoretical charge distribution calculated using a 6-31G** basis set. There are also differences from the previous work in the procedures used for the analysis of the experimental data and the comparison of experimental and theoretical results.

The X-ray structure determination

(*a*) *Experimental*

Enraf–Nonius CAD-4 diffractometer, graphite-monochromated Mo $K\alpha$ radiation ($\lambda = 0{\cdot}7107$ Å). Crystal $0{\cdot}40 \times 0{\cdot}40 \times 0{\cdot}25$ mm grown from aqueous solution with {110} and {001} forms, mounted with the $\mathbf{c}^*$ direction inclined about 4° from the φ axis of the diffractometer. Crystal cooled to 123 ± 2 K by a stream of liquid nitrogen gas from an Enraf–Nonius low-temperature device; temperature of crystal measured using a thermocouple about 8 mm upstream from the crystal. Unit-cell parameters obtained by a least-squares fit to $\sin^2\theta$ values of 30 reflections with $12° < \theta < 28°$ measured at $\pm\theta$. There is satisfactory agreement between present X-ray and previously reported X-ray and neutron values (Table 1, SCM).

Integrated intensities measured for a sector in reciprocal space hkl, with $h \geq k$ and $\sin\theta/\lambda < 1{\cdot}15$ Å^{-1}; $\theta/2\theta$ scans, variable scan width $\Delta 2\theta = (2{\cdot}2 + 0{\cdot}7\tan\theta)°$; a maximum of 300 s spent on each reflection.‡ Three reflections remeasured after every 25 reflections: variations in intensity within 3%. Integrated intensities were estimated from the scan profiles, which were recorded at 96 equal intervals, using the Lehmann–Larsen algorithm as modified for X-ray data by Blessing, Coppens & Becker (1974). For weak reflections where this method failed, the

† Present address: University of Western Australia, Nedlands, WA 6009, Australia.

‡ The crystal was lost before a second sector could be measured.

0108-7681/84/040398-07$01.50

backgrounds were assumed to be the first and last sixths of the total scan. Because the effects of X-ray absorption on the relative intensity data were estimated to be less than 1% ($\mu = 1{\cdot}07\ \text{cm}^{-1}$), no corrections were applied. Of the 612 measured reflections, 318 with $|F_o| > 3\sigma(F_o)$ were used in the structure determination.

(b) The X-ray structure refinement

Structure refinements based on a multipole pseudoatom model (Stewart, 1976) carried out with a full-matrix least-squares program (Craven & Weber, 1982); $\sum w\Delta^2$ minimized where $\Delta = |F_o^x| - |F_m^x|$ and $w = \sigma^{-2}(F_o^x)$.* Each pseudoatom was represented by an invariant component consisting of a Hartree–Fock isolated C, N, or O atom or contracted H atom with atomic scattering factors taken from Cromer & Waber (1965) or Stewart, Davidson & Simpson (1965). The pseudoatom asphericities and departure from electrostatic neutrality were represented by variable electron population parameters applied to terms involving single Slater-type radial and multipole angular functions. The explicit functions for C, N, O and H atoms were the same as those given by Epstein, Ruble & Craven (1982). Initially, fixed standard values of 3·4, 3·9, 4·5 and 2·5 bohr^{-1} (the Bohr radius is 52·92 pm) (Hehre, Stewart & Pople, 1969) were used for the radial exponent α of C, N, O and H atoms respectively. The fixed neutron values of SCM were used for all atomic positional parameters and for the H-atom thermal parameters.

The X-ray refinement began using 46 variables consisting of the scale factor, an isotropic extinction parameter assuming type I extinction with Lorentzian mosaicity (Becker & Coppens, 1974), 10 anisotropic thermal parameters and 34 electron population parameters. The refinement converged with the sum of the monopole populations for the asymmetric unit equal to −0·15 (8) e, as compared with the zero value expected for the net charge of a neutral molecule. The scale factor was then eliminated as an independent variable by the constraint that the net charge should indeed be zero. Also the extinction parameter was eliminated since the value $g = 0{\cdot}025\,(9) \times 10^4\ \text{rad}^{-1}$ was considered to be insignificantly different from zero. With 44 variables, there was convergence with $R_w = 0{\cdot}013$, $R = 0{\cdot}033$ and $S = 1{\cdot}36$. It was noted that values for the anisotropic thermal parameters of the OCN_2 group were in good agreement with the corresponding values obtained by neutron diffraction (see Table 4 of SCM). A refinement was then carried out with fixed SCM neutron values for all positional and thermal parameters, so that the variables consisted only of the 34 electron population parameters. Convergence was obtained with $R_w = 0{\cdot}015$, $R = 0{\cdot}035$ and $S = 1{\cdot}53$.

At this stage, the results of the theoretical calculations became available, leading to the X-ray structure refinements I_x and II_x.† They form the basis for most of the discussion and comparisons which are to be presented here. In both these refinements, the scale factor, k, for the X-ray structure amplitudes was obtained by a least-squares fit so as to minimize the residual $\sum w\delta^2$ where $\delta = |F_o^x| - (|F_o^t|/k)$ and $w = \sigma^{-2}(F_o^x)$. Compared with the previous value, which had been constrained to give a neutral urea molecule, the scale factor became 2% smaller. After the revised scale factor was applied to $|F_o^x|$, there was good overall agreement with $|F_o^t|$ ($R_w = 0{\cdot}023$). When average values ($\langle|F_o^t|\rangle/\langle|F_o^x|\rangle$) were calculated for reflections in shells with increasing $\sin\theta/\lambda$, the values were close to 1·0 except for a decrease at $\sin\theta/\lambda > 1{\cdot}0\ \text{Å}^{-1}$, the minimum value being 0·8 for the 12 reflections with $\sin\theta/\lambda > 1{\cdot}1\ \text{Å}^{-1}$. Possibly, the neglect of thermal diffuse scattering has caused $|F_o^x|$ to be overestimated for these reflections.‡

In the X-ray refinement I_x, the structure model was as before, except for the rescaling of $|F_o^x|$, the only variables being the 34 electron population parameters. Convergence was obtained with $R_w = 0{\cdot}015$, $R = 0{\cdot}035$ and $S = 1{\cdot}57$. In the final difference Fourier synthesis (Fig. 1*a*), the most significant residual electron density (−4·0 σ) is the trough near the N atom.

In the X-ray structure refinement II_x, the only difference from I_x was a change in the fixed values used for the four radial exponents α. The standard values of Hehre *et al.* (1969) were replaced by those obtained from the theoretical structure refinement II_t (see below). With these α values, refinement II_x gave convergence with $R_w = 0{\cdot}015$, $R = 0{\cdot}035$ and $S = 1{\cdot}53$. In the final difference Fourier synthesis (Fig. 1*b*), there is no significant residual density. The electron population parameters from both refinements I_x and II_x are given in Table 1. The charge density deformation maps calculated from these pseudoatom parameters (including p_v) are shown in Figs. 2 and 3.

* Refinement criteria were $R = (\sum|\Delta|/\sum|F_o^x|)$; $R_w = [\sum w\Delta^2/\sum w(|F_o^x|)^2]^{1/2}$ and $S = [\sum w\Delta^2/(n_{\text{obs}} - n_{\text{param}})]^{1/2}$. The following are superscripts or subscripts used throughout to denote electron density distributions ρ, or structure amplitudes $|F|$: x: experimental, based on X-ray data; n: experimental, based on the SCM neutron diffraction data; t: theoretical, based on quantum-chemical calculations for urea assuming the SCM nuclear geometry and thermal motion; i: theoretical, based on an assumed distribution of independent neutral Hartree–Fock atoms; o: assumed observation in a least-squares refinement; m: derived from a pseudoatom multipole model.

† Lists of observed ($|F_o^x|$ and $|F_o^t|$) and calculated structure factors and the electron population parameters with respect to crystal axes have been deposited with the British Library Lending Division as Supplementary Publication No. SUP 39253 (17 pp.) Copies may be obtained through The Executive Secretary, International Union of Crystallography, 5 Abbey Square, Chester CH1 2HU, England.

‡ For urea, this does not appear to have a serious effect on the atomic thermal parameters. There are no systematic differences in values obtained from the neutron data (used for $|F_o^t|$) and those obtained in the initial refinement based on $|F_o^x|$.

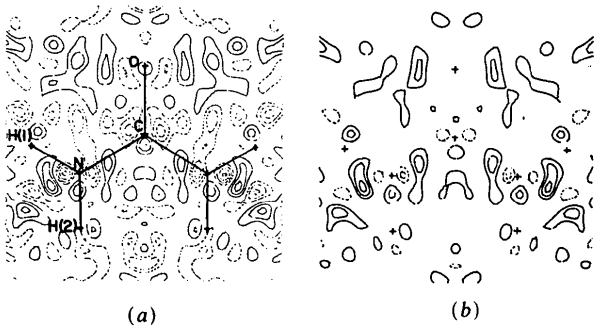

Fig. 1. Difference Fourier synthesis showing the residual charge density ($\rho_o^x - \rho_m^x$). Contours are at intervals of 0·05 e Å^{-3} with negative regions shown as dotted lines and with the zero contour omitted. The e.s.d. in the residual charge density is 0·05 e Å^{-3}. (*a*) Refinement I_x. (*b*) Refinement II_x.

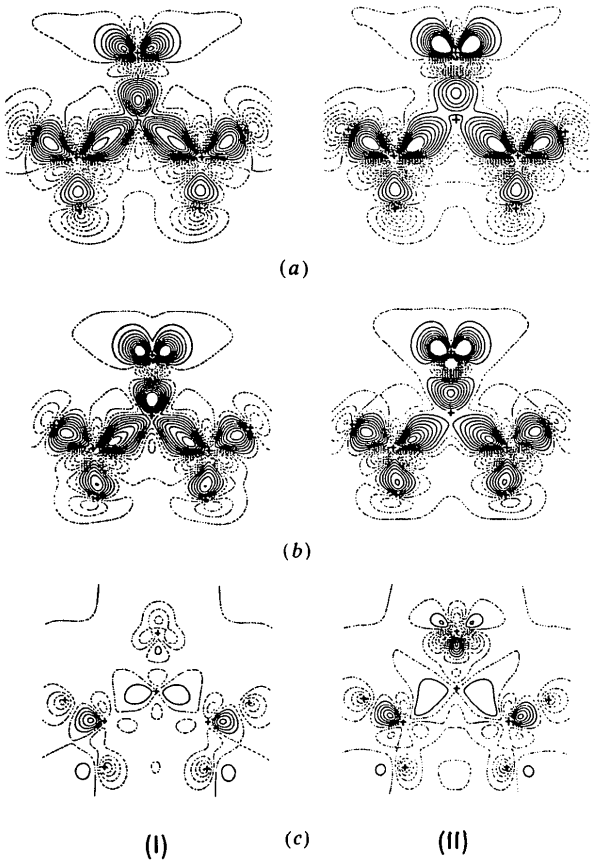

Fig. 2. The deformation density for atoms at rest calculated from the pseudoatom model. Contours are at intervals of 0·1 e Å^{-3} with the zero contour and regions of electron deficiency shown as dotted lines. Sections on the left are from refinement I and on the right from II. (*a*) Pseudoatom model fitted to the X-ray structure amplitudes, $|F_o^x|$. The largest features are +1·5 (3) and −0·9 (2) e Å^{-3} near the O atom for II_x. (*b*) Pseudoatom model fitted to the theoretical structure amplitudes, $|F_o^t|$. The largest features are +1·5 (3) and −1·4 (2) e Å^{-3} near the O atom for II_t. (*c*) The difference map, (*a*)–(*b*). Because of the large e.s.d. near the O atom (0·36 e Å^{-3}) only the differences near the H atoms are significant.

(*c*) *Fourier synthesis of the dynamical charge density distribution*

Because of good agreement in the anisotropic thermal parameters of the OCN_2 group determined by X-ray and neutron diffraction, we were encouraged to calculate the deformation charge density by the $X-N$ method (Coppens, 1974). Thus, Fig. 4(*a*) is a difference Fourier synthesis with coefficients ($|F_o^x| - |F_i^n|$) and phases α_i. Here, $|F_i^n|$ values are the X-ray structure amplitudes for an assembly of neutral isolated atoms with anisotropic thermal parameters determined by neutron diffraction, and α_i are the corresponding phase angles for this model. There were no significant differences from Fig. 4(*a*) when the difference Fourier synthesis was calculated with the same coefficients but with phases α_m derived from the multipole refinement (I_x). It seems reasonable to assume that the lack of detail in Fig. 4(*a*) compared with the static charge distribution (Figs. 2, 5) is due to the atomic thermal motion which is expressed in $|F_o^x|$ and $|F_i^n|$. However, this is only partly true, as can be seen from the comparison of Fig. 4(*a*) with the doubly phased map, Fig. 4(*b*), in which $|F_o^x|$ has the phase α_m from the multipole least-squares refinement (I_x) and $|F_i^n|$ has the phase α_i. In Fig. 4(*b*), many features are enhanced by a factor of at least two in magnitude, and additional detail emerges.

As discussed in detail by Stewart & Spackman (1984), serious limitations must be expected when conventional $X-N$ or $X-X$ Fourier methods are employed for charge density studies of noncentrosymmetric crystal structures such as urea. These

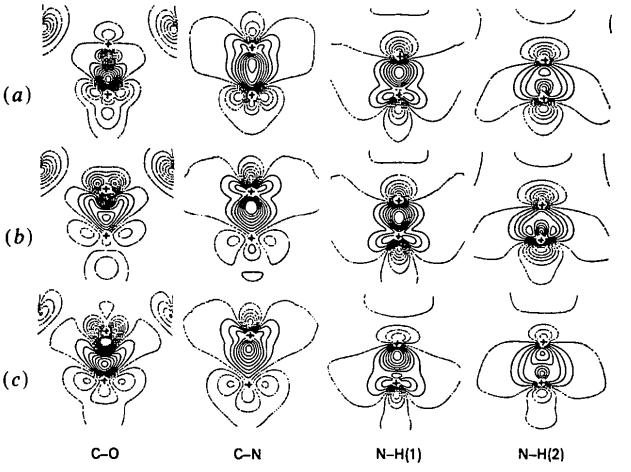

Fig. 3. The static deformation density calculated from the pseudoatom model in sections through the bonds and normal to the molecular plane. In each section the bond direction is shown vertical with atom C below O in C–O, and so on. Contours are as in Fig. 2. (*a*) Pseudoatoms fitted to the X-ray structure amplitudes, refinement I_x. (*b*) Pseudoatoms fitted to the X-ray structure amplitudes, refinement II_x. (*c*) Pseudoatoms fitted to the theoretical structure amplitudes, refinement II_t.

Table 1. *Electron population parameters* ($\times 10^2$)

The population parameters are normalized (Epstein, Ruble & Craven, 1982) and are referred to a Cartesian molecular axial system with x along the twofold symmetry axis C → O, and y along the normal to the molecular plane given by the vector product (C → O) × (C → N). In this system, the population parameters for the dipole d_2, quadrupoles q_2, q_4 and octopoles o_2, o_4, o_6 are zero for all atoms because of crystallographic symmetry. Values denoted by I_x and I_t come from least-squares refinements using the same pseudoatom model (I) but with observed structure amplitudes derived from the X-ray data $|F_o^x|$ or from the theoretical wavefunction $|F_o^t|$, respectively. For these refinements the standard values assumed for the radial exponents were $\alpha = 3{\cdot}4$, $3{\cdot}9$, $4{\cdot}5$ and $2{\cdot}5$ bohr^{-1} for C, N, O and H pseudoatoms. In refinement II_n with the radial exponents as additional variables, values $\alpha_C = 2{\cdot}34\,(4)$, $\alpha_N = 4{\cdot}22\,(10)$, $\alpha_O = 5{\cdot}07\,(15)$ and $\alpha_H = 2{\cdot}60\,(9)$ bohr^{-1} were obtained, and were then used as fixed values in refinement II_x.

		p_v	d_1	d_3	q_1	q_3	q_5	o_1	o_3	o_5	o_7
	I_x	4 (6)	8 (2)	0	18 (4)	0	12 (2)	16 (8)	0	−32 (4)	0
	I_t	−12 (4)	13 (2)	0	26 (2)	0	7 (2)	12 (8)	0	−30 (2)	0
	II_x	28 (4)	18 (4)	0	30 (5)	0	18 (3)	35 (5)	0	−58 (7)	0
	II_t	18 (6)	30 (2)	0	50 (2)	0	0 (2)	28 (3)	0	−62 (5)	0
O	I_x	1 (3)	10 (2)	0	−6 (4)	0	10 (2)	1 (2)	0	10 (2)	0
	I_t	10 (2)	11 (2)	0	−4 (2)	0	12 (2)	6 (6)	0	8 (2)	0
	II_x	−12 (2)	10 (1)	0	−3 (2)	0	10 (3)	6 (2)	0	18 (8)	0
	II_t	−18 (2)	13 (2)	0	−1 (2)	0	16 (2)	6 (2)	0	8 (4)	0
N	I_x	−15 (5)	1 (2)	−4 (4)	−9 (1)	−4 (3)	4 (2)	2 (2)	1 (4)	27 (10)	3 (2)
	I_t	−17 (4)	2 (2)	−8 (3)	−7 (1)	−5 (3)	0 (2)	2 (3)	3 (4)	24 (8)	−6 (2)
	II_x	−21 (4)	0 (2)	−2 (3)	−7 (1)	−2 (3)	3 (2)	6 (2)	1 (3)	30 (6)	0 (2)
	II_t	−23 (3)	2 (1)	−6 (3)	−6 (1)	−4 (3)	−2 (2)	1 (2)	1 (3)	20 (4)	−3 (2)
H(1)	I_x	−14 (3)	−9 (2)	−24 (4)	−6 (5)	12 (4)	6 (2)				
	I_t	1 (2)	−16 (2)	−20 (3)	4 (2)	14 (4)	9 (3)				
	II_x	−15 (2)	−9 (1)	−22 (2)	−5 (3)	15 (3)	0 (2)				
	II_t	−1 (2)	−12 (1)	−19 (2)	4 (2)	16 (3)	7 (2)				
H(2)	I_x	−14 (3)	21 (2)	4 (3)	12 (5)	−2 (3)	−7 (2)				
	I_t	0 (2)	21 (2)	−6 (3)	9 (2)	−1 (4)	−14 (3)				
	II_x	−15 (2)	19 (1)	2 (2)	10 (3)	−4 (3)	−4 (2)				
	II_t	−1 (2)	19 (1)	−5 (2)	8 (2)	−3 (3)	−13 (2)				

limitations arise because phases having unrestricted values (0 to 2π) are inadequately determined when the conventional isolated neutral-atom model is assumed.

Theoretical calculations

An *ab initio* theoretical wavefunction was determined with the closed-shell restricted Hartree–Fock self-consistent field method, using the program *GAUSSIAN*82 (Binkley *et al.*, 1983), with the 6-31G** basis set (Hariharan & Pople, 1973; Hehre, Ditchfield & Pople, 1972; Ditchfield, Hehre & Pople, 1971). This basis set, which is more extensive than the 4-31G set used in an earlier calculation by Scheringer *et al.* (1978), includes *d* functions on the C, N and O atoms, and *p* functions on the H atoms. The geometry of the isolated urea molecule used for the calculation is from the nuclear positional coordinates of SCM at 123 K (Table 3). Although the calculation of the wavefunction does not take into account the intermolecular interactions in the crystal structure, they are implicit to the extent that the geometry is that of a molecule removed from the crystal without any nuclear relaxation.

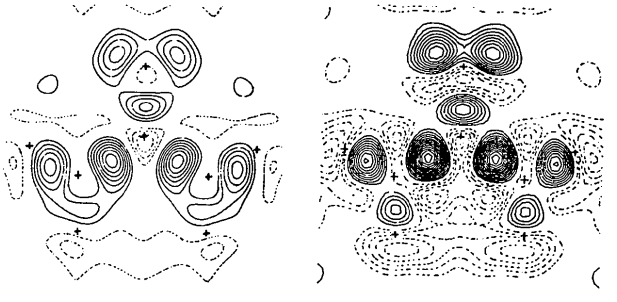

(*a*) (*b*)

Fig. 4. Difference Fourier sections showing dynamical deformation densities by the $(X - N)$ method. All atomic positional and thermal parameters were determined from neutron diffraction. Contours are at intervals of 0·05 e Å^{-3} with the zero contour omitted. (*a*) Phases for $(|F_o^x| - |F_i^n|)$ obtained assuming spherical neutral atoms. (*b*) Phase for $|F_o^x|$ determined from the pseudoatom refinement I_x and for $|F_i^n|$ assuming spherical neutral atoms.

Fig. 5 displays the theoretical deformation electron density for atoms at rest, $(\Delta\rho^t)_{stat} = (\rho^t - \rho_i^t)_{stat}$ where ρ_i^t is the superposition of isolated spherically averaged atomic electron densities. We avoid basis-set truncation effects by subtracting spherically averaged atomic densities obtained from open-shell unrestricted Hartree–Fock wavefunctions using the 6-31G basis set (*i.e.* excluding polarization functions).

A set of structure factor amplitudes $|F_o^t|$ on an 'absolute' scale was calculated from the 6-31G** wave function assuming a crystal composed of such isolated molecules arranged as in the crystal structure of urea at 123 K. The Fourier transforms on Gaussian-orbital products were calculated with the algorithm of Chandler & Spackman (1978). Thermal motion was included in an approximate manner, by applying the neutron anisotropic temperature factors of SCM to the atomic cores and by assuming a rigid-rod model for two-center products (Stewart, 1969).

A least-squares refinement I_t was then carried out in which $|F_o^t|$ values were treated as the observations and the structure model was assumed to be the same as that which was used in the X-ray structure

refinement I_x.† In particular, this involved the same set of neutral spherical atomic cores, and the same set of multipole and radial functions, assuming standard values for the radial exponents, α. However, since the observations were considered to be free of error, all reflections were assigned weights equal to the multiplicity of the reflection. The refinement (I_t) converged with $R = 0{\cdot}012$. The static deformation density calculated from this pseudoatom model (Fig. 2*b*, I_t) and from the wavefunction (Fig. 5) are in qualitative agreement, but with some significant differences. Thus the positive and negative features along the C–O bond are $+1{\cdot}0\,(1)$ and $-0{\cdot}7\,(1)$ e Å^{-3} in Fig. 2(*b*) (I_t) and $+0{\cdot}67$ and $-1{\cdot}36$ e Å^{-3} in Fig. 5.

A second refinement II_t was then carried out with the same pseudoatom model except that the radial exponents were included as four additional variables. This gave convergence with $R = 0{\cdot}009$. The pseudoatom parameters for refinements I_t and II_t (Table 1) show notable differences in the α values, particularly for the C atom. After refinement II_t, the deformation density along the C–O bond (Fig. 2*b*, II_t) agrees very well [$+0{\cdot}7\,(1)$ and $-1{\cdot}4\,(1)$ e Å^{-3}] with Fig. 5. However, a comparison of Figs. 3 and 5 shows other differences near the C and N atoms which may be significant. The final difference Fourier syntheses for I_t and II_t (not shown) are featureless except for sharp troughs centered at the O, N, and C atoms ($-0{\cdot}25$, $-0{\cdot}20$, $-0{\cdot}15$ e Å^{-3}, respectively).

† Calculations were performed independently with the least-squares refinement programs of Stewart & Spackman (1983) and Craven & Weber (1982). The residual $\sum w\Delta^2$ was 14% smaller when using the former program, which takes into account terms with second derivatives of the structure amplitudes (Spackman & Stewart, 1984). However, there were no significant differences in R values or electron population parameters.

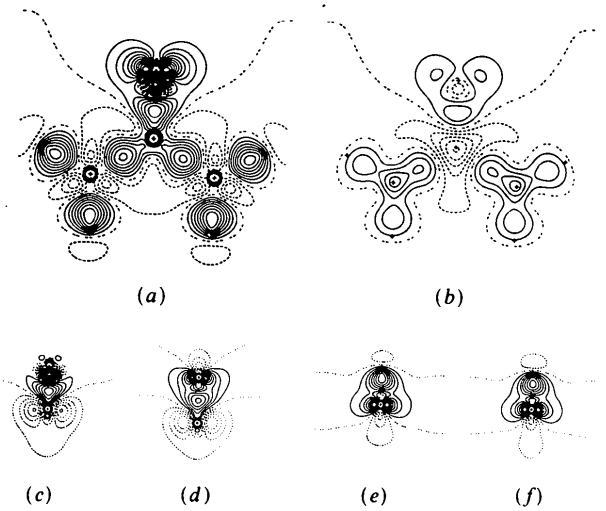

Fig. 5. Static deformation density for an isolated urea molecule calculated from the 6-31G** wavefunction. Contours are at intervals of $0{\cdot}1$ e Å^{-3} with dotted contours for regions of deficient electron density. (*a*) Section in the molecular plane. (*b*) Section 0·4 Å above the molecular plane. (*c*) Section through the C–O bond normal to the molecular plane; the nuclear sites are shown as (+), the lower being the C atom. (*d*) As in (*c*) for the C–N bond. (*e*), (*f*) Sections for N–H(1), N–H(2) with the N atom being the lower.

Discussion

In crystallographic studies of charge density there are advantages in using structural models which aim for a complete quantitative description of the charge density distribution as well as the nuclear positions and thermal vibrations. In principle, this approach enables the direct comparison of a theoretical distribution of deformation charge density such as Fig. 5 to be made with an experimental distribution free from the effects of thermal motion and phase-angle uncertainties which can be seen in Fig. 4. For such structure models, it is important to have an assessment of their merits and limitations. In the case of the rigid pseudoatom model, the approximations and assumptions which are involved have been discussed (Stewart, 1976). The model has also been applied in the study of a variety of simple molecular crystal structures, but without extensive testing. For urea at 123 K, two variants (I and II) of a simple pseudoatom model have been fitted by least squares, both to the experimental X-ray diffraction data ($|F_o^x|$) and to the corresponding data ($|F_o^t|$) for a simulated crystal structure based on an accurate wave function for the isolated molecule. This enables comparisons of pseudoatom electron population parameters (Table 1) and deformation densities (Figs. 2, 3) to be made with each other and with the deformation density from the wavefunction (Fig. 5).

The most obvious differences between the model maps (Figs. 2, 3) and the theoretical map (Fig. 5) are in the peak shapes. The peaks tend to be more rounded in Fig. 5. These differences are attributed to the truncation of the multipole expansion which is used to describe the asphericity of each pseudoatom. Because of practical limitations on the number of electron population parameters to be determined, the multipole expansion is carried as far as octopole terms for C, N and O atoms and quadrupoles for H atoms. This appears to be adequate for organic molecules where the pseudoatoms have approximate trigonal or tetrahedral site symmetry.

There are also differences in the magnitude of some features in the static deformation densities obtained from the wavefunction and from the simulated crystal structure. These are attributed to the nature of the assumed radial functions in the pseudoatom model. In both models which were tested (I and II), each multipole angular term is associated with a single Slater-type radial function (Epstein, Ruble & Craven, 1982) having a radial exponent (α) with the same value for all terms involving pseudoatoms of the same

kind (C, N, O or H). Except for H-atom monopole terms, these radial functions are zero at the pseudoatom nucleus. With increasing distance from the nucleus r, the radial functions used for C, N and O atoms increase to a maximum at $r=(n/\alpha)$ a.u., ($n=3$ for octopole terms, otherwise $n=2$), and then decrease more slowly. For α in the range of interest for urea (5·0 to 2·0 bohr^{-1}) and for $n=2$, the maximum occurs with $0{\cdot}2<r<0{\cdot}5$ Å (Fig. 6). At $r=1{\cdot}0$ Å, the radial function is reduced to 1% of the maximum value when $\alpha=5{\cdot}0$ bohr^{-1} and to 60% when $\alpha=2{\cdot}0$ bohr^{-1}. Thus with decreasing α, the pseudoatom becomes more diffuse and more effective in describing charge density features further from the nucleus.

In model I, standard α values (Hehre, Stewart & Pople, 1969) were assumed. The resulting monopole population parameters (P_l in Table 1) correspond to a net positive charge for the urea molecule of 0·34 (8) e which is close to the ideal zero value. Since there are 32 electrons in urea, 98·9% are accounted for by model I. Also, the molecular charge distribution is partitioned so that the net charges on individual pseudoatoms are consistent with intuitive notions of electronegativity. The O atom has an excess of 0·12 (2) electrons while the C atom has a marginal deficiency of 0·12 (4). However, as described in *Theoretical calculations*, model I results in significant differences in the deformation densities derived from the simulated crystal structure (Fig. 2) and the wave function (Fig. 5), particularly along the C–O bond. The standard α values, which were derived from energy-minimization calculations for selected isolated small molecules, might not be optimal for the spatial fitting of the charge density deformations in urea. Accordingly, in model II, the four α values were included as least-squares variables in the refinement involving the simulated crystal structure. There were considerable changes. Most notably, the C atom becomes more diffuse with a reduction in α from 3·4 to 2·34 (4) bohr^{-1} and the O atom more contracted, with α increasing from 4·5 to 5·07 (15) bohr^{-1}. Model II leads to an improvement in overall agreement with the deformation density distribution in Fig. 5. The differences are within 0·2 e Å^{-3}, except for the mirror-related peaks flanking the N atom in Fig. 3(*c*) and Fig. 5(*d*) where the difference is 0·6 (1) e Å^{-3}. The N-atom environment has, in addition to these sharp peaks at a distance 0·2 Å from the nucleus (Fig. 5*d*), features centered in the molecular plane at distances 0·4, 0·7 and 0·8 Å (Fig. 5*a*). It appears that these features cannot all be well fitted with a model involving such a restricted radial function. Other consequences in assuming model II are that the net charge of the molecule (from P_l, Table 1) involves a deficiency [0·50 (8) e] marginally greater than for model I, and there are also reversals in the net charges of the C and O pseudoatoms. The C atom expands and acquires a marginal excess of 0·18 (6) e while the O atom contracts and becomes electron deficient by 0·18 (2) e. These results demonstrate the dependence of pseudoatom charges on the nature of their radial functions. Comparisons of net charges should be restricted to pseudoatoms of the same kind. Thus in urea, according to both models I and II, there is no significant difference in the charge on H(1) and H(2).

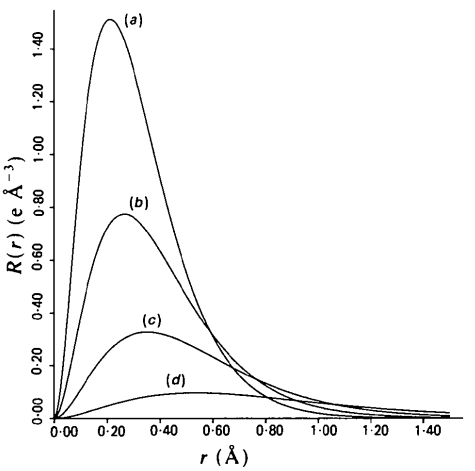

Fig. 6. The normalized one-electron radial function $R(r)=(\alpha^5/96\pi)r^2\exp(-\alpha r)$ plotted for four values of the radial exponent, $\alpha=5$, 4, 3, 2 bohr^{-1}. These are shown as (*a*), (*b*), (*c*) and (*d*) respectively. This radial function is of the form used for monopole, dipole and quadrupole terms of C, N and O pseudoatoms.

Although there are limitations, the simple pseudoatom models I and II are effective in reproducing most features of the theoretical deformation density for urea. On the basis of the above comparisons and earlier theoretical studies of X-ray scattering by first-row diatomic hydrides (Bentley & Stewart, 1975), it appears that the model would best be improved by choosing more flexible radial functions for the C, N and O deformation terms. Such improvements will be the subject of future studies.

As might be expected, when the pseudoatom models I and II are fitted to the experimental diffraction data for urea, the results are very similar to those obtained from the simulated diffraction data. With the experimental data, the electron deficiency for the entire molecule increases to 0·81 (11) and 0·86 (8) for models I and II, so that only 97·5 and 97·3% of the total number of electrons are taken into account. The most significant differences in the model deformation density maps (Fig. 2*c*) may be real, since they are associated with the H atoms. It should be noted that the molecules are extensively H-bonded in the real crystal structure, whereas the wavefunction and the simulated crystal structure are based on the isolated molecule. As seen in the monopole population parameters (Table 1) both H(1) and H(2) have a deficiency of 0·14 (3) electrons compared with the

isolated molecule. Also, at each H atom (Fig. 2*c*) the region of electron depletion is not centered at the nucleus, but rather is extended towards the O atom with which it is H-bonded.* These features are consistent with theoretical calculations which indicate that H bonding is primarily an electrostatic interaction (Morokuma, 1977).

It is concluded that when used to reveal the effects of chemical binding, the simple pseudoatom model is about equally efficient when applied either to the experimental $|F_o^x|$ or to the theoretical $|F_o^t|$ structure amplitudes.

The pseudoatom model has recently been applied in crystallographic charge density studies of other molecules containing the ureide group. These include parabanic acid at room temperature (Craven & McMullan, 1979) and 123 K (He, Swaminathan, Craven & McMullan, 1984), barbital at 198 K (Craven, Fox & Weber, 1982), and alloxan at 123 K (Swaminathan, Craven & McMullan, 1984*b*). The detailed comparison and discussion of these results is deferred.

We are grateful to Dr Michael J. Frisch for assistance with the *GUASSIAN* 82 calculations, and to Mrs Joan Klinger for technical assistance. This work was supported in part by Grants GM-22548 from the National Institutes of Health and CHE80-16165 from the National Science Foundation.

* Symmetry-related H(2) atoms in the same molecule are both H-bonded to the same O atom which lies along the c direction on the twofold axis.

References

BECKER, P. J. & COPPENS, P. (1974). *Acta Cryst.* A**30**, 129–147.
BENTLEY, J. & STEWART, R. F. (1975). *J. Chem. Phys.* **63**, 3794–3803.
BINKLEY, J. S., FRISCH, M J., DEFREES, D. J., RAGHAVACHARI, K., WHITESIDE, R. A., SCHLEGEL, H. B., FLUTER, G. & POPLE, J. A. (1983). *GAUSSIAN* 82. Chemistry Department, Carnegie–Mellon Univ., Pittsburgh, PA.
BLESSING, R. H., COPPENS, P. & BECKER, P. (1974). *J. Appl. Cryst.* **7**, 480–492.
CHANDLER, G. S. & SPACKMAN, M. A. (1978). *Acta Cryst.* A**34**, 341–343.
COPPENS, P. (1974). *Acta Cryst.* B**30**, 255–261.
CRAVEN, B. M., FOX, R. O. & WEBER, H. P. (1982). *Acta Cryst.* B**38**, 1942–1952.
CRAVEN, B. M. & MCMULLAN, R. K. (1979). *Acta Cryst.* B**35**, 934–945.
CRAVEN, B. M. & WEBER, H. P. (1982). *The POP Least Squares Refinement Procedure.* Tech. Rep. CC-74. Crystallography Department, Univ. of Pittsburgh, Pittsburgh, PA 15260.
CROMER, D. T. & WABER, J. T. (1965). *Acta Cryst.* **18**, 104–109.
DITCHFIELD, R., HEHRE, W. J. & POPLE, J. A. (1971). *J. Chem. Phys.* **54**, 724–728.
EPSTEIN, J., RUBLE, J. R. & CRAVEN, B. M. (1982). *Acta Cryst.* B**38**, 140–149.
HARIHARAN, P. C. & POPLE, J. A. (1973) *Theor. Chim. Acta*, **28**, 213–222.
HE, X., SWAMINATHAN, S., CRAVEN, B. M. & MCMULLAN, R. K. (1984). In preparation.
HEHRE, W. J., DITCHFIELD, R. & POPLE, J. A. (1972). *J. Chem. Phys.* **56**, 2257–2261.
HEHRE, W. J., STEWART, R. F. & POPLE, J. A. (1969). *J. Chem. Phys.* **51**, 2657–2664.
MOROKUMA, K. (1977). *Acc. Chem. Res.* **10**, 294–300.
MULLEN, D. (1980). *Acta Cryst.* B**36**, 1610–1615.
MULLEN, D. & HELLNER, E. (1978). *Acta Cryst.* B **34**, 1624–1627.
SCHERINGER, C., MULLEN, D., HELLNER, E., HASE, H. L., SCHULTE, K. W. & SCHWEIG, A. (1978). *Acta Cryst.* B**34**, 2241–2243.
SPACKMAN, M. A. & STEWART, R. F. (1984). *Acta Cryst.* Submitted.
STEWART, R. F. (1969). *J. Chem. Phys.* **51**, 4569–4577.
STEWART, R. F. (1976). *Acta Cryst.* A**32**, 565–574.
STEWART, R. F., DAVIDSON, E. R. & SIMPSON, W. T. (1965). *J. Chem. Phys.* **42**, 3175–3187.
STEWART, R. F. & SPACKMAN, M. A. (1983). *Valray Users Manual.* Department of Chemistry, Carnegie–Mellon Univ., Pittsburgh, PA.
STEWART, R. F. & SPACKMAN, M. A. (1984). Unpublished.
SWAMINATHAN, S., CRAVEN, B. M. & MCMULLAN, R. K. (1984*a*). *Acta Cryst.* B**40**, 300–306.
SWAMINATHAN, S., CRAVEN, B. M. & MCMULLAN, R. K. (1984*b*). *Acta Cryst.* Submitted.

Acta Cryst. (1984). B**40**, 404–417

Nonbonded Potentials for Azahydrocarbons: the Importance of the Coulombic Interaction

BY DONALD E. WILLIAMS AND STEVEN R. COX

Department of Chemistry, University of Louisville, Louisville, Kentucky 40292, *USA*

(*Received* 9 *August* 83; *accepted* 6 *December* 1983)

Abstract

A transferable nonbonded N···N potential of the (exp − 6 − 1) type was obtained by fitting the crystal structure of α-nitrogen (N_2) and nine crystal structures of azahydrocarbon molecules which do not exhibit hydrogen bonding: ethanedinitrile (C_2N_2), ethylenetetracarbonitrile (C_6N_4), *cis*-1,2,3-cyclopropanetricarbonitrile ($C_6H_3N_3$), 1,1,2,2-cyclopropanetetracarbonitrile ($C_7H_2N_4$), triethylenediamine ($C_6H_{12}N_2$), hexamethylenetetramine ($C_6H_{12}N_4$), pyrimidine ($C_4H_4N_2$), pyrazine ($C_4H_4N_2$), and β-

0108-7681/84/040404-14$01.50